

Supporting Information for

Metal-Vacancy-Solid-Solution NiAlP Nanowall Array Bifunctional Electrocatalyst for Exceptional All-pH Overall Water Splitting

Weiren Cheng^{1,†}, Hui Zhang^{1,†}, Xu Zhao¹, Hui Su¹, Fumin Tang¹, Jie Tian² and Qinghua Liu^{1,*}

¹ National Synchrotron Radiation Laboratory, University of Science and Technology of China, Hefei 230029, Anhui, P. R. China

² Material Test and Analysis Lab, Engineering and Materials Science Experiment Center, University of Science and Technology of China, Hefei 230026, Anhui, P. R. China

†These authors contributed equally to this work.

*E-mail: qhliu@ustc.edu.cn

S1. Materials

Synthesis of NiAl_δP Nanowall Arrays. NiAl-LDH precursor was solvothermally synthesized on Ni foam, which was pre-cleaned by concentrated HCl and washed by acetone and water. Then the as-prepared NiAl-LDH precursor was treated by alkali-etching and phosphorization processes to form the final NiAl_δP nanowall array. In a typical synthesis, 0.5 mmol of Ni(NO₃)₂·6H₂O, 0.5 mmol of Al(NO₃)₃·9H₂O, and 0.25g cetyltrimethylammonium bromide (CTAB) were dissolved in a mixed solution of 3 ml distilled water and 15 ml methanol under stirring to form a clear solution. A piece of the pre-treated Ni foam (1 cm × 3 cm) was immersed in a 25 ml Teflon-lined autoclave containing above mixture solution. The autoclave was sealed and maintained at 150 °C for 20 h, and then it was cooled down naturally to room temperature. After that, the sample was washed with distilled water and ethanol several times, and then was immersed into 3M KOH solution for 12 h. Subsequently, the alkali-etching sample was placed in the reaction chamber along with 0.5 g NaH₂PO₂ towards heating treatment for 4 h under vacuum environment, where NaH₂PO₂ and alkali-etching sample was put in the high-temperature section of 300 °C and low-temperature section of 100 °C, respectively, to obtain the black color NiAl_δP

nanowall array formed on Ni foam. The pristine NiAlP nanowall array was synthesized in a similar method without alkali-etching process.

S2. Materials characterization

Transmission electron microscopy (TEM), high-resolution TEM (HRTEM), and energy dispersive X-ray spectroscopy (EDS) measurements were performed on a JEM-2100F microscope in Material Test and Analysis Lab, Engineering and Materials Science Experiment Center, University of Science and Technology of China (USTC). The field emission scanning electron microscopy (SEM) images was taken on a FEI Sirion-200 scanning electron microscope. The X-ray diffraction (XRD) patterns were performed on Philips X'Pert Pro Super X-ray diffractometer with Cu $K\alpha$ radiation. X-ray photoelectron spectra (XPS) were acquired at the photoemission end-station at beamline BL10B in the National Synchrotron Radiation Laboratory (NSRL) in Hefei, China. The beamline is connected to an undulator and equipped with two gratings that offer soft X-rays from 100 to 1000 eV with a typical photon flux of 5×10^{10} photons/s and a resolution ($E/\Delta E$) better than 10^3 at 244 eV. The binding energies obtained in the XPS spectral analysis were corrected for specimen charging by referencing C 1s to 284.5 eV.

Electrochemical measurements were performed using an electrochemical workstation (Model CHI760D, CH instruments, Inc., Austin, TX) with a standard three-electrode electrochemical cell and was used to record catalytic activity of samples in various solutions, where the as-prepared samples, a gauze platinum and Ag/AgCl (saturated KCl) act as the working, auxiliary, and reference electrode, respectively. Also, the overall water splitting performance of samples were performed using the same electrochemical workstation with a two-electrode-cell, where the as-prepared samples act as both cathode and anode electrode. For comparison, the commercial catalyst powders (20 wt% Pt/C and RuO₂) were loaded on a pretreated NF with loading mass of 2.0 mg cm⁻² via drop casting of catalyst ink. The catalyst ink, was a 1 mL ethanol solution consisting of 5 mg of catalyst powder, 5 μ L of Nafion (5%, Sigma Aldrich), 200 μ L of ethanol, and

795 μL of distilled water. Tafel plots were obtained from the extrapolation of the linear region of a plot of overpotential versus current density. Chronopotentiometric measurements was recorded at $j=10 \text{ mA cm}^{-2}$ for 20 h. Cyclic voltammetry curves were measured in the region of 1.10–1.40 V at various scan rates (20, 40, 60 mV S^{-1} , etc.) for the calculation of the double-layer capacitance (C_{dl}). All the final potentials were calibrated with respect to a reversible hydrogen electrode (RHE). The hydrogen and oxygen evolved from the cathode and anode in two-electrode-cell could be measured by a water-gas displacing method in the second hour of durability test.

The volume of H_2 and O_2 were calculated from the following relationships:¹

$$V_{\text{H}_2} \text{ mL} = Q \text{ C} \times 22.4 \text{ L mol}^{-1} \times 1000 / (F \text{ C mol}^{-1} \times 2)$$

$$V_{\text{O}_2} \text{ mL} = Q \text{ C} \times 22.4 \text{ L mol}^{-1} \times 1000 / (F \text{ C mol}^{-1} \times 4)$$

Where Q is the cumulative charge (C), F is the Faraday constant (C mol^{-1}).

The TOF values were calculated according to the following formula:²

$$\text{TOF} = \text{total hydrogen (oxygen) turn overs per cm}^{-2} / \text{surface active sites per cm}^{-2}$$

Note that the total number of the surface sites (including metal and phosphorus atoms) was estimated as the number of the active sites from the electrochemical surface area together with the unit cell of the catalysts. Taking NiAlP as an example, the upper limit of the surface active sites per real surface area can be calculated to be $\sim 2.03 \times 10^{15}$ atoms per cm^2 real surface area.

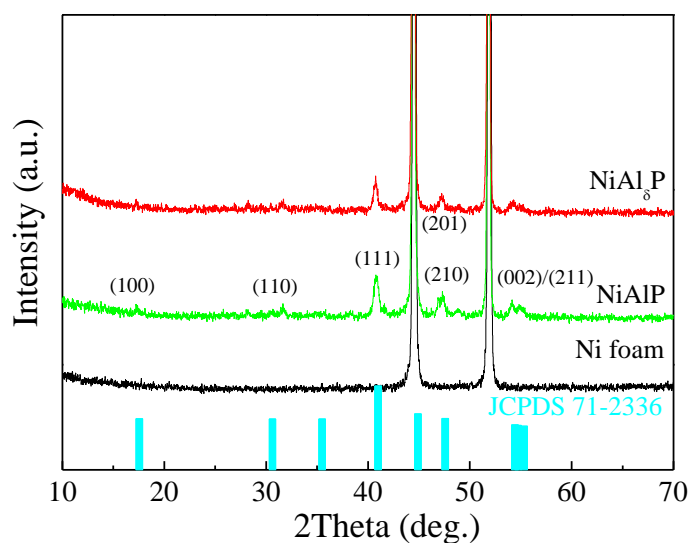


Figure S1. XRD patterns of Ni foam, NiAlP and NiAl₅P nanowall arrays.

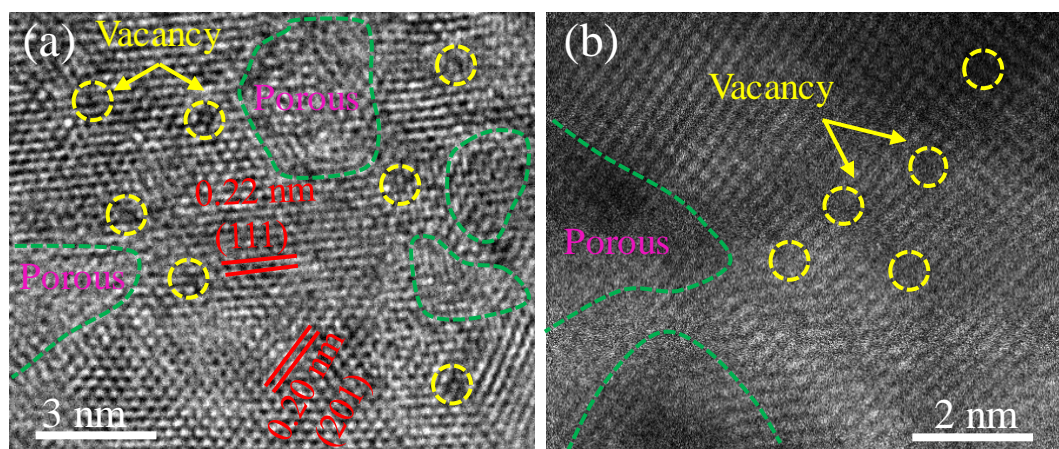


Figure S2. (a) HRTEM image and (b) HAADF-TEM image for NiAl₅P nanowall arrays.

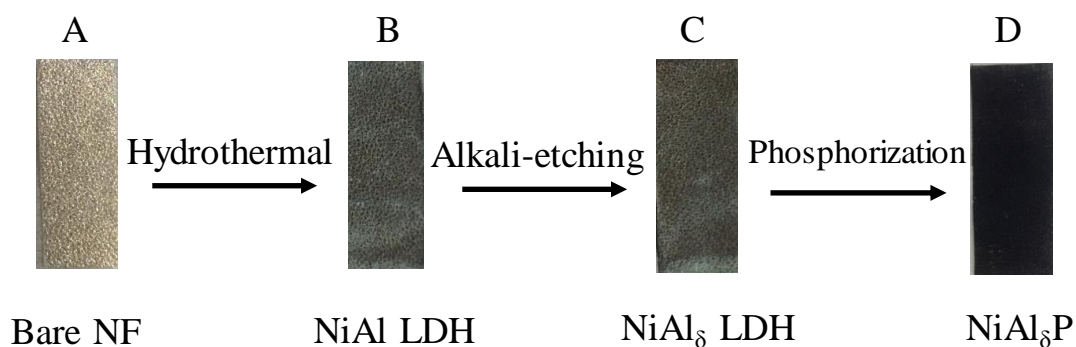


Figure S3. The photographic images of (A) Ni foam (NF), (B) NiAl LDH, (C) etched NiAl₅ LDH and (D) NiAl₅P nanowall arrays.

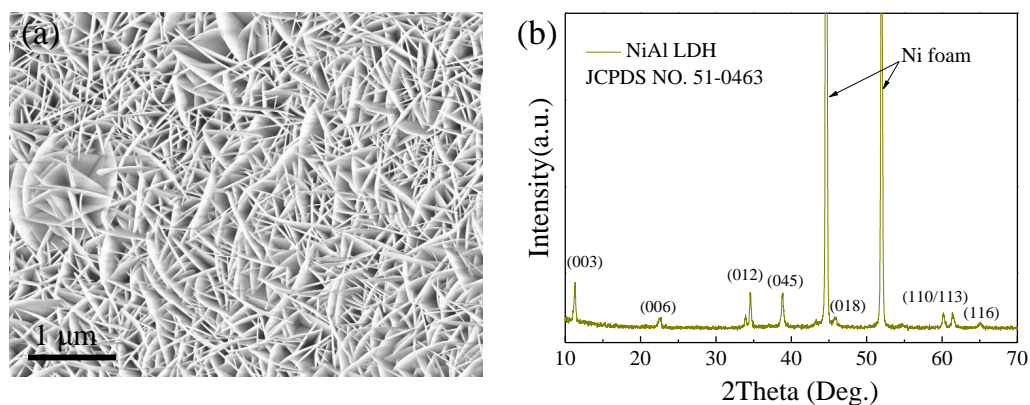


Figure S4. (a) SEM image and (b) XRD pattern for NiAl LDH.

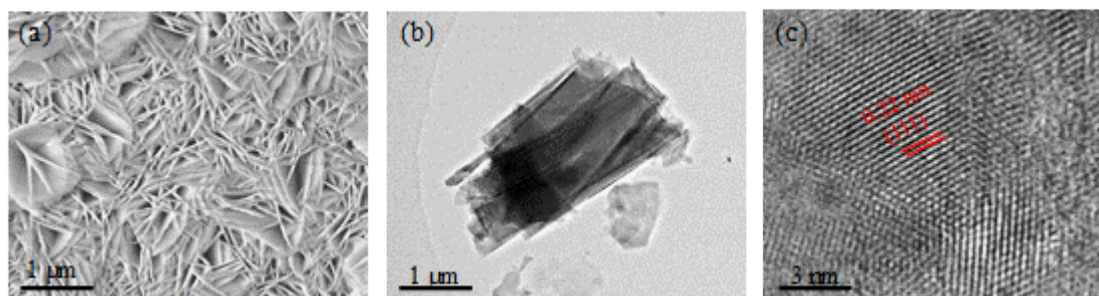


Figure S5. (a) SEM image, (b) TEM image, and (c) HRTEM image for NiAl₅P nanowall arrays.

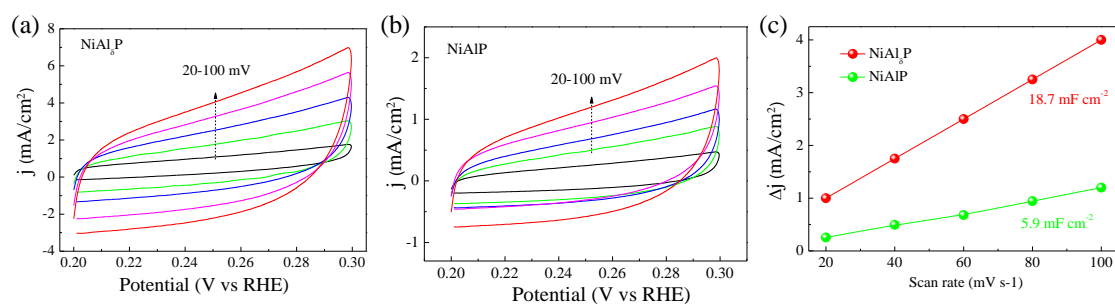


Figure S6. CV measurements for (a) NiAl₅P and (b) pristine NiAlP nanowall arrays and (c) double-layer capacitances for NiAl₅P and NiAlP nanowall arrays towards HER active surface area.

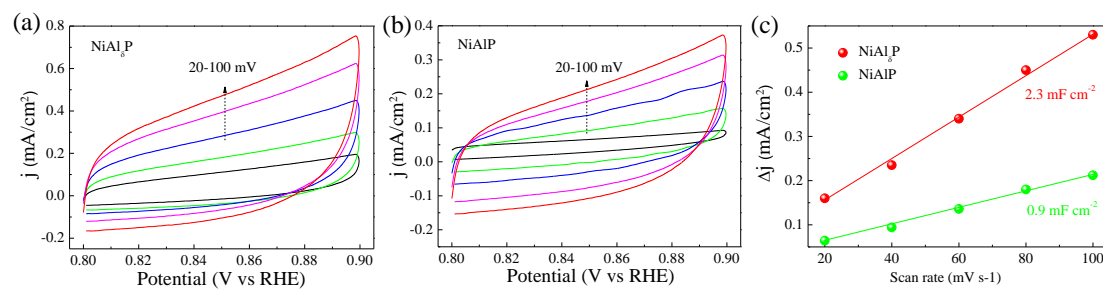


Figure S7. CV measurements for (a) NiAl₅P and (b) pristine NiAlP nanowall arrays and (c) double-layer capacitances for NiAl₅P and NiAlP nanowall arrays towards OER active surface area.

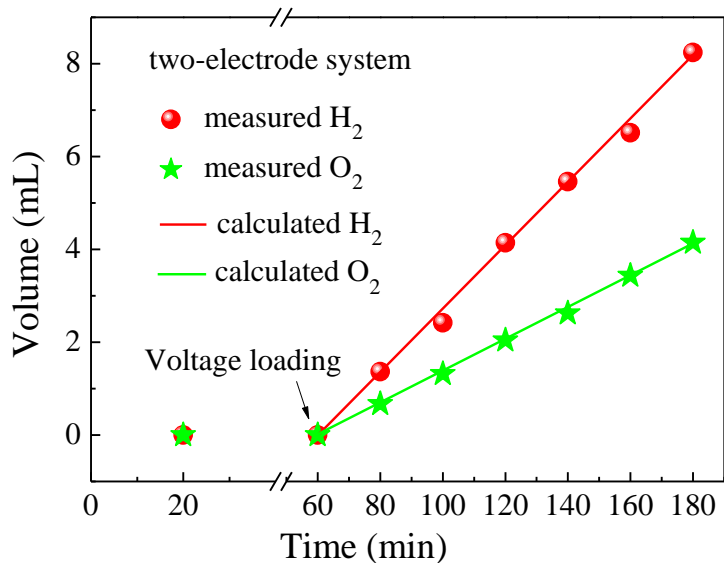


Figure S8. Generated H₂ and O₂ volumes over time versus theoretical quantities assuming ~100% Faradaic efficiency calculated from corresponding current density for overall water splitting in a two-electrode-cell.

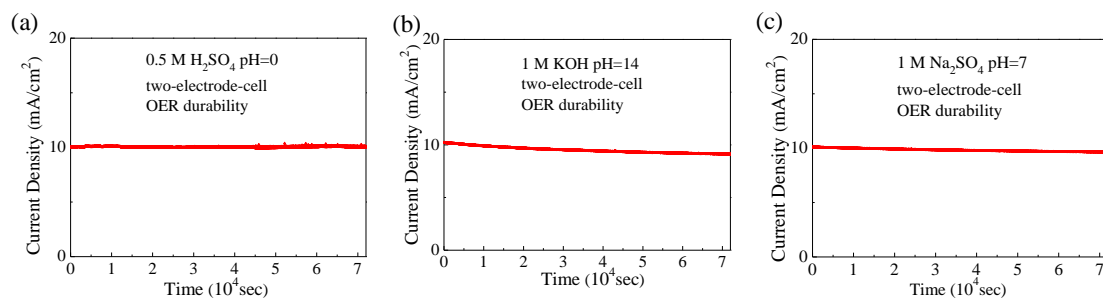


Figure S9. Time-dependent current density of NiAl₃P nanowall arrays in (a) 0.5 M H₂SO₄, (b) 1M KOH, and (c) 0.5M Na₂SO₄ solutions.

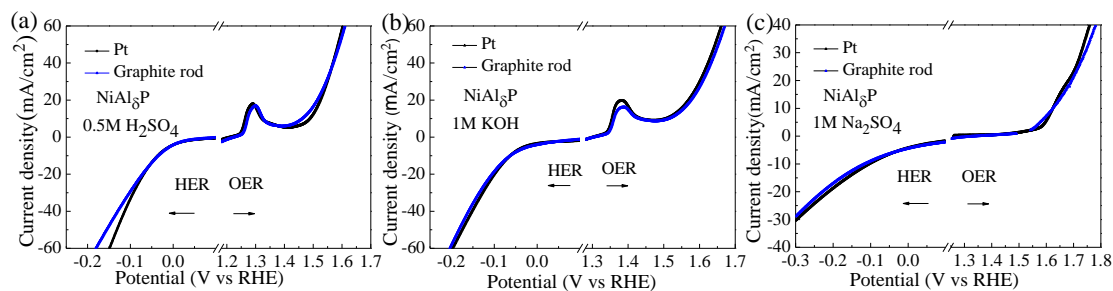


Figure S10. Electrocatalytic activity tests for NiAl₃P nanowall arrays in acidic (a), basic (b), and neutral solution (c) with Pt and graphite rod as counter electrode.

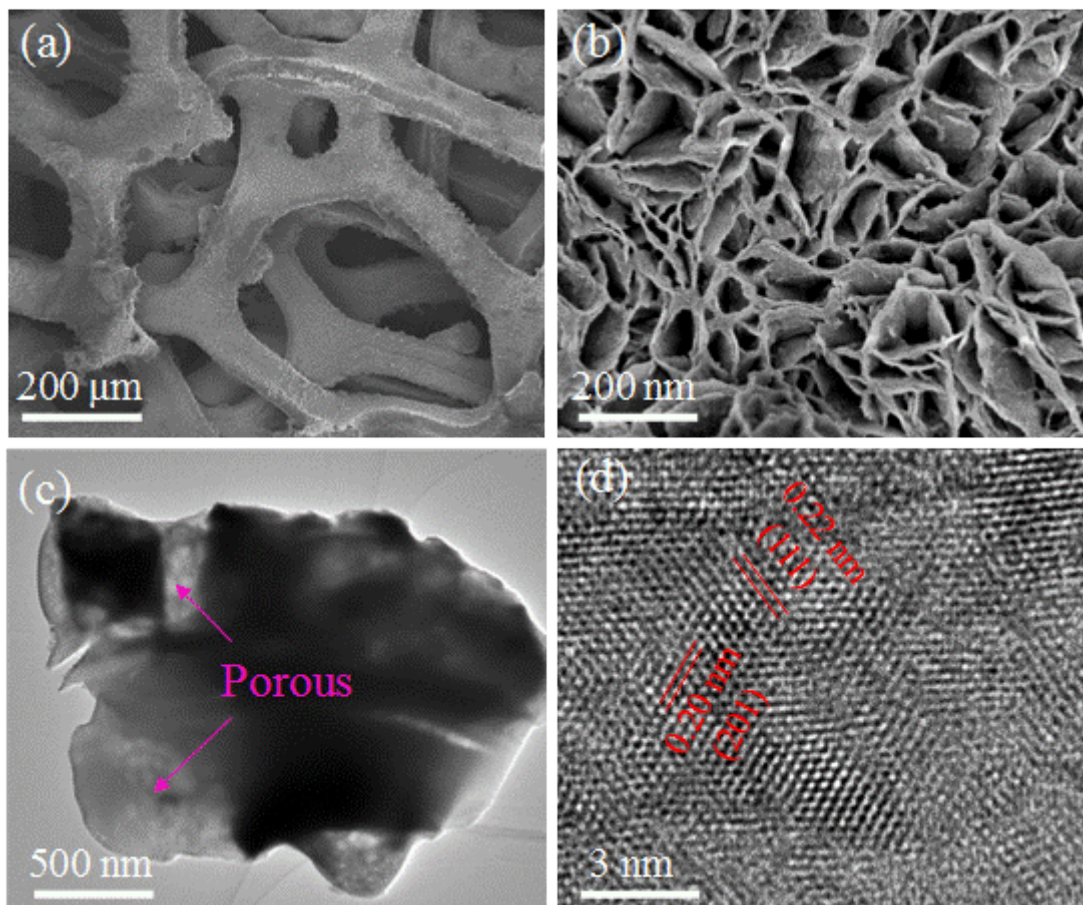


Figure S11. (a) SEM image, (b) enlarged SEM image, (c) TEM image, and (d) HRTEM image for NiAl₃P nanowall arrays after catalytic tests in 0.5 M H₂SO₄.

Table S1. A comparative summary of overall water splitting performance for most reported earth-abundant bifunctional electrocatalysts.

Catalysts	Electrolyte	Cell voltage (V) at 10 mA cm ⁻²	(Ref.)
NiCoP	1M KOH	1.58	Nano Lett. 2016, 16, 7718–7725
Ni-P/NF	1 M KOH	1.64	J. Mater. Chem. A 2016, 4, 5639
Ni ₂ P/NF	1M KOH	1.63	Energy Environ. Sci. 2015, 8, 1027
Co-P/Cu foil	1M KOH	1.65	Angew. Chem. Int. Ed. 2015, 54, 6251
CoP/CoP ₂	1 M KOH	1.65	Nanoscale, 2017, 9, 5677–5685
NiSe/NF	1M KOH	1.63	Angew. Chem. Int. Ed. 2015, 54, 9351
CoSe ₂ /CC	1M KOH	1.63	Adv. Mater. 2016, 28, 7527.
IrCoNi	0.5 M H ₂ SO ₄	1.64	Adv. Mater. 2017, 1703798
NiFe LDH/NF	1M KOH	1.70	Science, 2014, 345, 1593
CoMn-CH	1M KOH	1.68	J. Am. Chem. Soc. 2017, 139, 8320–8328
NiAl ₃ P/NF	0.5M H ₂ SO ₄	1.52	This work
NiAl ₃ P/NF	1M KOH	1.55	This work
NiAl ₃ P/NF	1M Na ₂ SO ₄	1.73	This work

Table S2. A comparative summary of HER performance in acidic electrolyte for the most reported earth-abundant electrocatalysts.

Catalysts	Electrolyte	Overpotential (mV) at -10 mA cm ⁻²	Tafel slope (mV dec ⁻¹)	(Ref.)
FeP	0.5 M H ₂ SO ₄	240	67	Chem. Commun., 2013, 49, 6656
Co-NRCNTs	0.5 M H ₂ SO ₄	260	80	Angew.Chem. Int. Ed., 2014, 53, 4372.
CoPNC	0.5 M H ₂ SO ₄	50	46	Nano Lett. 2015, 15, 7616–7620
Ni/NiO/CoSe ₂	0.5 M H ₂ SO ₄	88	39	Angew. Chem. Int. Ed. 2013, 52, 8546.
NiCoSe MNSN/NF	0.5 M H ₂ SO ₄	52	39	Adv. Mater. 2017, 29, 1606521
MoS ₂ /CoSe ₂	0.5 M H ₂ SO ₄	68	36	Nat. Commun. 2015, 6, 5982
WS _{2(1-x)} Se _{2x} /NiSe ₂	0.5 M H ₂ SO ₄	88	47	Nano Lett. 2016. 16, 7604
NiSe ₂ nanosheet	0.5 M H ₂ SO ₄	117	32	Angew. Chem. Int. Ed. 2016, 128, 7033.
MoSe ₂ /carbon paper	0.5 M H ₂ SO ₄	250	~60	Nano Lett. 2013, 13, 3426.
NiAl ₃ P/NF	0.5M H ₂ SO ₄	35	38	This work
NiAl ₃ P/NF	1M KOH	80	52	This work
NiAl ₃ P/NF	1M Na ₂ SO ₄	100	93	This work

Table S3. A comparative summary of OER performance in various electrolytes for most reported earth-abundant catalysts.

Catalysts	Electrolyte	Overpotential (mV) at -10 mA cm ⁻²	Tafel slope (mV dec ⁻¹)	(Ref.)
NiCoP/NF	1M KOH	280	87	Nano Lett. 2016, 16, 7718–7725
Ni ₂ P	1KOH	290	47	Energy Environ. Sci. 2015, 8, 2347
Ni-P/C	1KOH	300	64	Energy Environ. Sci. 2016, 9, 1246
CoP	1KOH	282	62	ChemSusChem 2016, 9, 472
FeP/carbon paper	1KOH	350	64	Chem. Commun. 2016, 52, 8711
CoMn LDH/NF	1KOH	324	43	JACS 2014, 136, 16481
FeCoW	1KOH	223	37	Science 2016, 352, 333
NiFeP	0.05 M H ₂ SO ₄	540	~100	Adv. Mater. 2017, 29, 1606570
IrNiCu/C	0.1 M HClO ₄	~300	48	ACS Nano 2017, 11, 5500–5509
NiAl ₅ P/NF	0.5M H ₂ SO ₄	256	76	This work
NiAl ₅ P/NF	1M KOH	242	65	This work
NiAl ₅ P/NF	1M Na ₂ SO ₄	400	103	This work

S3. DFT calculation details

The first-principles density functional theory (DFT) calculations were performed using a plane wave basis set with the projector augmented plane-wave (PAW) method.^{3,4} The exchange-correlation interaction was described within the generalized gradient approximation (GGA) in the form of PW91.⁵ The energy cutoff was set to 400 eV, and the atomic positions were allowed to relax until the energy and force were less than 10^{-4} eV and 10^{-2} eV/Å, respectively. A $11 \times 11 \times 11$ k-mesh was employed for the Brillouin zone integrations. All calculations were performed on a slab model with 2×2 surface cell, containing four (0001) atomic layers and a vacuum layer of 15 Å thickness to avoid artificial interaction between periodic images. The top and bottom layers were allowed to relax, while the middle two layers were fixed.

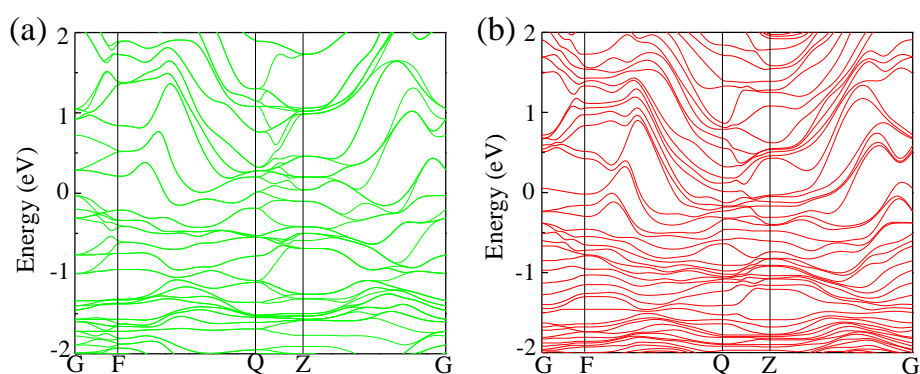


Figure S12. Theoretical band structures of (a) NiAlP and (b) NiAl₅P.

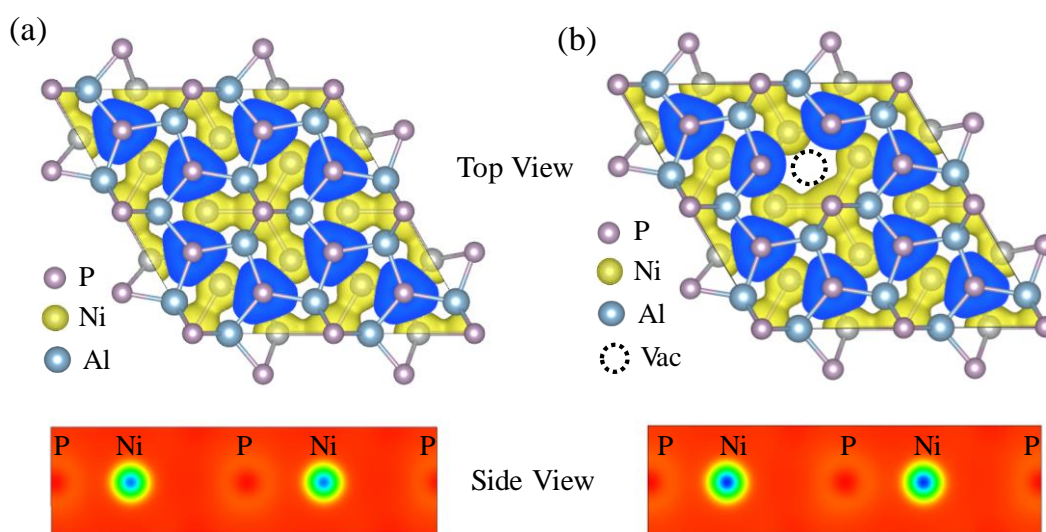


Figure S13. Calculated local charge densities of (a) NiAlP and (b) NiAl₅P.

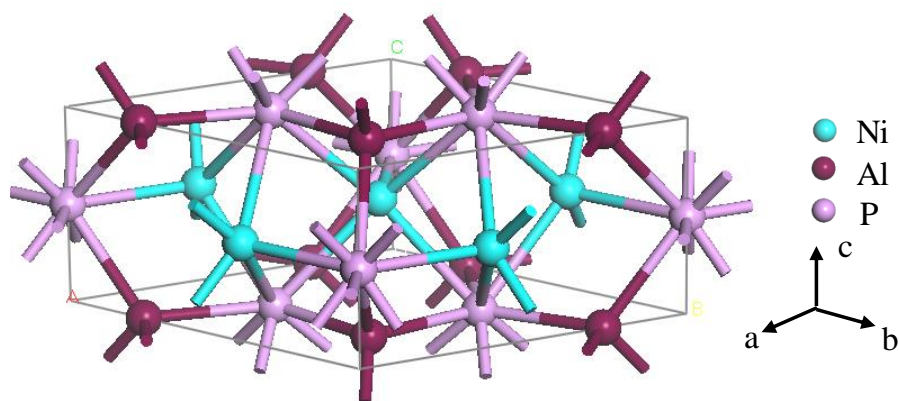


Figure 14. The side view of NiAlP model.

It can be seen that NiAlP lattice, with lattice parameter of $a=b=5.834 \text{ \AA}$ and $c=3.351 \text{ \AA}$ ($\alpha=\beta=90^\circ$, $\gamma=120^\circ$), consists of stacked Ni-P plane and Al-P plane along c axis.

References

1. Chen, G. F.; Ma, T. Y.; Liu, Z. Q.; Li, N.; Su, Y. Z.; Davey, K.; Qiao, S. Z. *Adv. Funct. Mater.* **2016**, *26*, 3314-3323.
2. Liang, H. F.; Gandi, A. N.; Anjum, D. H.; Wang, X. B.; Schwingenschlögl, U.; Alshareef, H. N. *Nano. Lett.* **2016**, *16*, 7718-7725.
3. Samanta, S.; Martha, S.; Parida, K. *ChemCatChem*, **2014**, *6*, 1453-1462.
4. Jiang J.; Yu, J.; Cao, S. W. *J. Colloid interface Sci.* **2016**, *461*, 56-63.
5. Furthmüller, G. K. *J. Comput. Mater. Sci.* **1996**, *6*, 15.